Second-harmonic generation in SiC polytypes

Sergey N. Rashkeev,* Walter R. L. Lambrecht, and Benjamin Segall
Department of Physics, Case Western Reserve University, Cleveland, Ohio 44106-7079
(Received 29 September 1997)

A first-principles study of the frequency-dependent second-harmonic generation (SHG) coefficients of various SiC polytypes ($2H$, $4H$, $15R$, $6H$, and $3C$), a group spanning the complete range of ''hexagonality,'' was carried out. It uses a recently developed computational approach based on the self-consistent linear muffin-tin orbital band-structure method, which is applied using the local-density approximation to density-functional theory with a simple *a posteriori* gap correction. The susceptibilies are obtained in the independent-particle approximation, i.e., without local-field effects. The zero-frequency limits of the ratio $\chi^{(2)}_{333}/\chi^{(2)}_{311}$ for the noncubic polytypes were found to be in excellent agreement with those obtained by the pseudopotential method (and in disagreement with simple geometric predictions), while the magnitudes of the individual components themselves were found to be smaller than the values earlier calculated. The spectral features of the full $\chi^{(2)}(-2\omega,\omega,\omega)$ for $2H$ are found to differ markedly from those of the other polytypes. The spectra in the series of decreasing degree of hexagonality ($4H$, $15R$, and $6H$) gradually approach those for the zinc-blende ($3C$) form. The independent tensorial components appearing in the rhombohedral but not in the hexagonal forms are found to be about a factor 6 smaller than the other ones. An analysis of the SHG spectra in terms of ω and 2ω resonances and individual band-to-band contributions is presented. It is suggested that second-harmonic generation spectra have an advantage over linear optical spectra for probing the electronic structure, particularly for the region within a few eV of the band edges in that they exhibit more detailed fine structure. That results from the sign variations in the products of matrix elements occurring in the SHG. [S0163-1829(98)01716-0]

I. INTRODUCTION

Recently, there has been a renewed interest in calculations of second-harmonic generation (SHG) and related nonlinear optical spectroscopies in semiconductors.[1–6] In a previous paper,[1] we presented our computational approach, which is based on the linear muffin-tin orbital band-structure method and the recent formulations of the problem of evaluating the second-order optical response functions for periodic solids in the independent-electron approximation by Sipe and Ghahramani[7] and Aversa and Sipe.[8] The independent-particle approximation band structures used in this work are based on the density-functional theory in the local-density approximation (LDA) with some *a posteriori* self-energy corrections to the gap.

In the course of our own and other's previous work,[1–6] a question that has attracted some interest is the influence of the crystal structure on the second-harmonic generation coefficients, in particular for materials that exhibit both the zinc-blende and the wurtzite structures. Of course, the number of independent elements and the relations between the nonvanishing elements of the second-order susceptibility tensor depend on the symmetry (cubic or hexagonal) of the crystal structure. In addition, on the basis of the strong similarity in the bonding, which is tetrahedral in both cases, one might expect there to be simple relations between the two tensorial components χ^h_{333} and χ^h_{113} in the hexagonal structure and the one nonvanishing component χ^c_{123} in the cubic structure, particularly in the static limit. These tensor relations are obtained simply by rotating the coordinate axes of the cubic coordinate system towards the hexagonal axes (z along [111] and x and y chosen in the {111} plane such that the hexagonal rings characteristic of both crystal structures are aligned) and are given by

$$\chi^h_{333} = -2\chi^h_{113} = 2\chi^c_{123}/\sqrt{3}. \tag{1}$$

Analogous relations have been used earlier for elastic constants.[9,10] While these simple geometric relations hold for the bond-orbital picture,[11] in which the total polarizability is a sum of local bond polarizabilities, they are not always well satisfied, as the near vanishing ratio of $\chi^h_{113}/\chi^h_{333}$ in wurtzite AlN demonstrates.[1,3,6] The response functions of concern describe the field-dependent polarizabilities of the electronic systems. These in turn are known to depend on the electronic structures which differ to a nontrivial extent in the different polytypes (e.g., they have different band gaps). Furthermore, the relation between SHG and the band structures is also far from trivial and involves fine details of the electronic structures, such as interband energy difference resonances and momentum matrix element products.

Silicon carbide would appear to be the material of choice for a further investigation of this question because of the occurrence of polytypes,[12] which are structures of varying degrees of ''hexagonality.'' A detailed review of recent progress in the understanding of the electronic structure and physical properties of the SiC polytypes can be found in Ref. 13 and other papers in the same volume. Specifically, ''hexagonality'' is defined as $H=h/(h+c)$, where h and c are, respectively, the number of hexagonal and cubic stackings in the elementary cell, a parameter that varies from zero for the cubic $3C$ form to unity for the purely hexagonal $2H$ polytype. Some other polytypes that are frequently encountered, either because of their natural abundance or because their growth has been optimized, are $6H$ ($H=1/3$) and $4H$ (H

$=1/2$). There exist also rhombohedral polytypes such as $15R$ ($H=2/5$). These have only threefold symmetry and thus have additional nonvanishing tensorial components, but we can still assign a hexagonality H to them as defined above.

In the static limit, Kleinman[14] ''permutation'' symmetry allows one to reduce the number of independent tensorial components beyond the relations dictated purely by crystallographic symmetry. Thus the 333 and 311 components fully describe the SHG susceptibility in the static limit. The ratio of $\chi^h_{311}/\chi^h_{333}$ in the static limit was studied previously for SiC polytypes by Chen *et al.*[5] Additional questions arise about (i) the magnitude of the nonvanishing tensor components of the rhombohedral polytypes and (ii) the validity of these relations for the frequency-dependent susceptibilities, including the additional independent tensorial components.

Some of these issues are investigated in this paper. Although we are at present unable to explain the magnitudes of the discrepancies from the expected geometric relations in simple terms, we can provide information on the general behavior of the frequency-dependent $\chi^{(2)}(-2\omega,\omega,\omega)$ susceptibility tensor as function of H. To this end we performed calculations of various tensor components of $\chi^{(2)}(-2\omega,\omega,\omega)$ for the $3C$, $6H$, $15R$, $4H$, and $2H$ SiC polytypes and we relate them to the corresponding linear-response function [more precisely to the imaginary part of the dielectric function $\varepsilon_2(\omega)$] and the calculated electronic band structures. The chosen group of polytypes encompasses the complete range of hexagonality.

The relation of SHG to the band structures is an important question in its own right. In fact, one may think of SiC polytypes as ''twist'' superlattices.[15] They consist essentially of narrow layers of cubic material bonded together with a 180° twist at the twin boundaries corresponding to the hexagonally stacked layers. The result of these twists is a frustration of the electron wave propagation.[16] This leads to standing-wave patterns which constitute essentially the ''miniband structure'' of the superlattice. In particular, the conduction-band structure near the band edges can be thought of in this manner and shows minigaps between folded cubic bands. Just as nonlinear optics is currently of great interest in more conventional compositionally modulated semiconductor superlattices (in particular those with polar interfaces), it is also expected to be of interest in the present context. Specifically, we will show that the second-harmonic generation spectrum in the range below the band gap but above half the band gap contains detailed information about the band structure. Measurements of these spectra in conjunction with the analysis presented here could thus provide experimental insight into these aspects of the polytype band structures. In that sense, the present work is closely related to our previous work on linear optical response functions,[13,17] which was also mainly concerned with the question of extracting as detailed as possible experimental information about the band structures from the optical data.

The SHG spectra appear to be more sensitive to the degree of hexagonality and to the underlying band structure than the corresponding linear response functions. There are two main reasons for that sensitivity. First, the second-order response involves more ''resonances'' than the linear one. In addition to the usual ω resonances the 2ω-resonant contributions appear. Second, the real and imaginary parts of the products of matrix elements that control the strength of a given resonance in $\chi^{(2)}$ can be positive or negative. In contrast, for the linear responses the corresponding factors involve only the square of matrix elements, which ensures, for example, that $\varepsilon_2(\omega)$ is positive. As a result, the structure in $\chi^{(2)}(-2\omega,\omega,\omega)$ is more pronounced than in the linear response. Hence measurements of the frequency-dependent nonlinear responses can in principle provide more detailed information about the electronic structure than those for the linear response. In that sense these measurements are similar to modulation spectroscopy techniques.[18] Another factor favoring the nonlinear studies is that the threshold for the 2ω part occurs at half the energy of threshold for linear processes. The measurements could thus be performed in a more convenient spectral region for the incident light. Although one still needs detection capabilities of the second harmonic in the doubled-frequency range, at least the intensity requirements for the incident light are thereby somewhat relaxed.

Unfortunately, at this point there has been only a very limited amount of experimental work on SHG in SiC in spite of the technological importance of this material. So far, there were measurements of the SHG only for the zero-frequency limit; some were carried out more than two decades ago.[19,20] Later there appeared some renewed experimental interest in such measurements and SHG in a cubic SiC film,[21] in a single crystal of polytype $6H$,[22] and in a pulsed laser ablated hexagonal SiC thin film[23] was measured. Very recently, Niedermeier *et al.*[24] carried out measurements of the anisotropy of the SHG on $3C$ SiC films on Si substrates and $6H$ and $15R$ crystals grown by the modified Lely method. At present, the primary interest of this work appears to be characterization of the quality of SiC samples. We hope that our present work will stimulate further interest in the more fundamental questions addressed here. In view of the absence of experimental studies of the frequency-dependent SHG, our first-principle calculations of the SHG have a predictive character.

The rest of the paper is organized as follows. In Sec. II we discuss our computational approach based on the linear muffin-tin orbital (LMTO) band-structure code. In Sec. III we analyze the results of calculations and find the main similarities and differences between the nonlinear responses for different SiC polytypes. A conclusion and summary of the results are presented in Sec. IV.

II. COMPUTATIONAL METHOD

The expressions used in the present work to calculate $\chi^{(2)}$ were given elsewhere.[1] They are a rearrangement of the formalism obtained by Sipe and Ghahramani,[7] and Aversa and Sipe[8] using the ''length-gauge'' formalism. Those results are based on the independent-particle approximation (meaning that no local-field effects are included) for undoped semiconductors, i.e., systems without partially filled bands. There are several advantages in using this formulation, namely, (i) the manifest absence of unphysical singularities in the zero-frequency limit, (ii) the simple and natural account of the effects of the intraband motion of electrons that gives an essential contribution to SHG, and (iii) the obvious satisfaction of the Kleinman relations[14] in the zero-frequency limit.

This formulation has recently been used successfully in two sets of studies. In one set Hughes *et al.* calculated $\chi^{(2)}(-2\omega,\omega,\omega)$ in GaAs and GaP,[2] which have the zinc-blende structure, and in GaN and AlN,[3] which form with the wurtzite structure. These calculations were based on band energies and momentum matrix elements obtained by the self-consistent full-potential linearized augmented-plane-wave band-structure method. The other set was carried out by the present authors,[1] who studied 3*C* SiC in addition to the above-mentioned four semiconductors. In those calculations we used the self-consistent method[25,26] LMTO within the atomic sphere approximation. The same approach will be used here. The method is very efficient mainly because it employs a rather small basis set. As a result it can more easily deal with systems containing a large number of atoms per unit cell while maintaining a sufficiently large number of **k** points so as to ensure converged Brillouin zone (BZ) integrations. Extensive checks performed in our other paper[1] demonstrate that our LMTO-based approach yields accurate results for the second-order response functions.

The self-consistent calculations of the electronic band structure (eigenvalues and eigenstates) were carried out within the framework of density-functional theory in the LDA (Ref. 27) using the exchange-correlation parametrization of Hedin and Lundquist.[28] As is extensively discussed in our other paper,[1] correcting for the well-known ''gap problem'' of the LDA is extremely important for nonlinear-response functions. While this is true even in the static limit, as can be justified from the point of view of the recently developed concept of polarization-dependent density-functional theory,[29] it is clearly imperative for frequency-dependent response functions to somehow deal with the actual quasiparticle excitations rather than the Kohn-Sham eigenvalues. One of the most accurate approaches presently available for the corrections to the LDA is the *GW* approximation.[30] However, calculation of the full energy-dependent and nonlocal self-energy operator even in this relatively simple approximation is rather cumbersome in practice because of the need for determining the fully dynamically screened Coulomb interaction *W*. A simplified approach is based on the observation that the conduction bands to a good approximation shift up rigidly in *GW* calculations. The effect can thus be described by a the so-called scissors operator, which can be written as a projection operator on the conduction bands times a constant shift in energy Δ. As was pointed out by Levine and Allan[4] and later by Hughes and Sipe,[2] the introduction of this shift operator into the Hamiltonian results in renormalization of the velocity (momentum) operator matrix elements. In practice, this renormalization factor is taken simply as

$$\mathbf{p}_{nm} \mapsto \mathbf{p}_{nm} \frac{\omega_{nm} + (\Delta/\hbar)(\delta_{nc} - \delta_{mc})}{\omega_{nm}}, \tag{2}$$

in which p_{nm} is a momentum matrix element between Bloch states n and m, $\hbar\omega_{nm} = E_n - E_m$ is their band difference, and the factor $\delta_{nc} - \delta_{mc}$ limits the corrections to matrix elements involving one valence and one conduction band. That approximation is based on the explicit assumption that the dipole moment r_{nm} matrix elements are unchanged because the perturbed wave functions are close to the LDA wave functions. In our other paper,[1] we noted some principle shortcomings of this approach in that it breaks the consistency between the eigenvalues and eigenvectors. We showed that better results were obtained by introducing the shift at the level of the LMTO Hamiltonian by an empirical modification of diagonal elements corresponding to the basis functions that primarily make up the conduction-band states. These typically are the cation and empty sphere *s*-like states for the lowest conduction bands in zinc-blende semiconductors. However, at present this approach only allows us to shift the lowest conduction bands rather than the whole set of conduction bands, which appears to be more appropriate for SiC. Also, a fine-tuning of this approach for SiC polytypes that are described using different empty spheres for the hexagonal and cubic local stackings remains to be carried out. In the interest of simplicity and a consistent treatment of all polytypes, we therefore here adopt the scissor's approach as described above.

The next question is what value of the constant shift Δ to adopt. The scissors approach gives a reasonable quantitative agreement with experiment for a variety of optical constants for moderately small-band-gap semiconductors when the value of Δ is straightforwardly taken to the difference between the experimental and LDA minimum band gaps. However, as was noted by Chen *et al.*[5] and by Gavrilenko and Bechstedt[31] the shifts required to reproduce the magnitude of the experimental dielectric constants $\varepsilon_1(0)$ for the SiC polytypes are less than the Δ needed to match the band gaps. Similar results occur for other large-band-gap semiconductors that contain second-row elements (B,C,N,O), i.e., the discrepancy in the LDA optical response functions are overcorrected by the use of the scissors approach.[5,6,29] In our opinion, this problem is further complicated by the effects of local-field corrections and continuum excitonic effects on the oscillator strength. Therefore, we think it is premature to attach too much importance to the magnitudes of the response functions, especially since we are presently not including local-field corrections. We prefer to focus on the energetic position of the spectral features. It was shown that a simple self-energy correction of about 1 eV for all the major SiC polytypes appears to bring the LDA values for the minimum gaps into good coincidence with experiment.[13] This value is well justified by recent calculations of such corrections using the *GW* approximation.[32–34] Also, a constant energy shift of $\varepsilon_2(\omega)$ by 1 eV leads to reflectivities in good agreement with measured reflectivity spectra[17] as far as the location of spectral features is concerned. Since our major interest for $\chi^{(2)}$ is also in the location of the spectral features, we therefore adopt the value $\Delta = 1$ eV. From our experience with other materials, we expect that both the use of the scissor operator approach in its present form and the choice of Δ may somewhat overestimate the correction to the LDA. We will keep this in mind when comparing to other values in the static limit. It should not affect our major conclusions about the spectral features. Local-field correction were shown to be not larger than 10% for the zero-frequency limit of $\chi^{(2)}$ in the SiC polytypes.[5] They are neglected in the present calculations.

Next, we turn to some computational details. The imaginary part of the frequency-dependent SHG is calculated first (see Ref. 1). The real part of the SHG is then obtained from

the Kramers-Kronig transformation. However, in the zero-frequency limit, the SHG can be evaluated with less effort by the use of a special expression. A comparison of that result with the limit of the frequency-dependent $\chi^{(2)}$ serves as a check of the accuracy of both the BZ integration and the Kramers-Kronig transformation. We note that the **k** integration can be limited to the irreducible wedge of the Brillouin zone only if a preliminary symmetrization of the product of the three momentum matrix elements over all the transformation of the crystal group is performed. For the frequency-dependent SHG, we use the usual tetrahedron scheme for the integrations with linear interpolation of the band energies and the products of the matrix elements. For the zero-frequency limit on the other hand, we employ a semianalytical linear interpolation scheme that is more efficient and produces a smaller error.[1]

Orbitals with angular moments up to $l_{max}=3$ were included in the basis set. As shown in other previous work[1] neglecting the f states leads to non-negligible errors in the momentum matrix elements and the SHG's.

We finish this section with a note on the symmetry-allowed tensorial components. In the cubic case, there is only one independent component, with indices 123, and all its possible permutations are equal to it (1, 2, and 3 refer to the x, y, and z axes, respectively, which are chosen along the cubic axes). In the hexagonal polytypes that correpond to the point group $6mm$, there are three independent components with indices 333, 311, and 131, the last one equaling the 113 component because for SHG the last two indices can always be permuted. The coordinate axes here are chosen with z along the sixfold symmetry axis. Furthermore, in the static limit the 311 and 131 components are equal by the Kleinman permutation symmetry, but this is no longer true for the frequency-dependent case. The rhombohedral polytype $15R$ (point group $3m$) has a threefold symmetry axis along the z axis, which is normal to the basal planes, instead of the sixfold screw axis present in the hexagonal structure. As a consequence of the lower symmetry there is one additional independent component of the SHG and several symmetry-related nonvanishing components. These are $\chi^{(2)}_{222}=-\chi^{(2)}_{211}=-\chi^{(2)}_{112}=-\chi^{(2)}_{121}$. As noted in the Introduction, a transformation of the $3C$ $\chi^{(2)}$ tensor from a cubic coordinate system to a hexagonal one (having the z axis along the cubic [111] direction) yields the 333, 311, and 131 components in terms of the 123 response function for $3C$. The resulting ratio $\chi^{(2)}_{333}/\chi^{(2)}_{311}=-2$ for arbitrary frequency ω. The -2 value found for the ratio when one uses directly computed components for $3C$ in the hexagonal coordinate system represents an additional verification of the computer code. One of the central questions of this paper is to what extent the same relation holds for the other polytypes.

III. RESULTS

A. Static limit

Since the zero-frequency limit of the SHG is simpler to calculate, it is the first aspect of the nonlinear response on which we will focus our attention. To put our own results in perspective, we briefly recall the history of static SHG results for SiC. One such calculation for SiC was carried out by

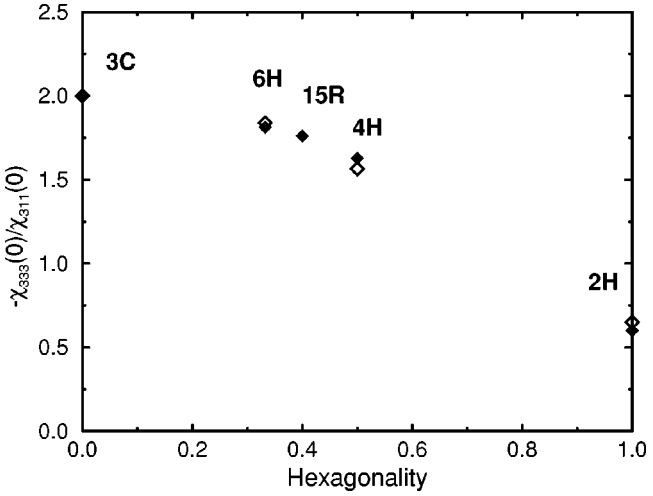

FIG. 1. Calculated ratio $-\chi^{(2)}_{333}(0)/\chi^{(2)}_{311}(0)$ as a function of hexagonality. The results of the present LDA calculations are shown as closed diamonds and those of Ref. 5 as open diamonds.

Levine using the bond-charge model.[11] He found that the $\chi^{(2)}_{123}$ in zinc-blende SiC and $\chi^{(2)}_{333}$ in wurtzite crystals are both negative. The subsequent analysis of the bond-charge model found that its predicted SHG values in SiC are very sensitive to the choice of the bond charge and the ion radii because both Si and C have the same ionic charge.[19] However, the ratio of the 333 and 311 tensor components in this model is found to be independent of the particular bond-charge model and to be equal to the above-mentioned value of -2 for all polytypes. For the $3C$ polytype, the ratio is purely geometric in origin. For this value to hold for the other polytypes, the approximation implied is one of similarity in the underlying electronic structure.

An indication that the real situation is more complicated and that the bond-charge model is not accurate at least for some hexagonal materials including nH SiC appeared in the work of Chen *et al.*[5,6] Our calculated ratios of the 333 and 311 components of $\chi^{(2)}$ for the zero-frequency limit are shown as a function of hexagonality in Fig. 1 along with the results of Chen *et al.*[5] It can be seen that the deviations for the noncubic forms increase with increasing hexagonality becoming substantial for the large values of H. Our values for the ratio are in excellent agreement with those obtained in the LDA pseudopotential calculations of Chen *et al.*,[5] which include local-field corrections. A comparison of the values of the individual 333 and 311 components obtained in the present and pseudopotential calculations is presented in Table I. It is seen that while there is good agreement for the ratios, the absolute LDA values of the $\chi^{(2)}$ appear to be more sensitive to the method of calculation. Those obtained by the LMTO method are found to be smaller than those by the pseudopotential approach. As expected, the gap corrections reduce the values in both our calculations and those of Chen *et al.* A slightly different value of the gap correction was used for each polytype in their case, with $1.04<\Delta<1.27$ eV.

Although there are non-negligible differences between our and their $\chi^{(2)}$ values, even in the LDA, we wish to point out that the two results agree much better with each other than with the bond-charge model predictions. The latter predict values independent of polytype, which in Ref. 11 are

TABLE I. LDA and LDA plus ''scissors'' calculations (with a 1-eV shift) of $\chi^{(2)}_{333}(0)$ and $\chi^{(2)}_{311}(0)$ compared with pseudopotential LDA calculations (in pm/V). The sign of the SHG's from Ref. 5 was adapted to the present choice of coordinate system (see the text).

Component	Method	$2H$	$4H$	$15R$	$6H$	∞H ($3C$)
$\chi^{(2)}_{333}(0)$	LDA	3.6	14.5	16.4	17.8	20.2
$\chi^{(2)}_{311}(0)$		-6.1	-8.9	-9.3	-9.7	-10.1
$\chi^{(2)}_{333}(0)$	LDA plus scissors	2.5	9.2	10.4	11.4	13.0
$\chi^{(2)}_{311}(0)$		-3.9	-5.7	-6.1	-6.3	-6.5
$\chi^{(2)}_{333}(0)$	LDA[a]	8.6	23.2		27.6	28.2
$\chi^{(2)}_{311}(0)$		-13.2	-14.8		-15.0	-14.2
$\chi^{(2)}_{333}(0)$	LDA plus scissors[a]	5.8	15.6		18.6	18.4
$\chi^{(2)}_{311}(0)$		-8.8	-10.0		-10.4	-9.2
$\chi^{(2)}_{333}(0)$	Expt.[b]		± 23			
$\chi^{(2)}_{311}(0)$			∓ 14			

[a]Reference 5.

[b]Rescaled from Ref. 19 for an undetermined α-SiC polytype; see the text.

$\chi_{333}=-166$ and $\chi_{311}=84$ pm/V. Singh *et al.*[19] pointed out that values about 10 times smaller, $\chi_{333}=-16$ and $\chi_{311}=8$ pm/V, are obtained when different ionic radii values are used as input to the same model. The two-band model prediction of Kleinman[35] gave $\chi_{333}=-80$ and $\chi_{311}=40$ pm/V. Note that all of these have opposite sign to ours. Experimentally, the values available correspond to an incompletely determined polytype[36] and are $\chi_{333}=\pm 27\pm 3$ and $\chi_{311}=\mp 15\pm 2$ pm/V at $\lambda=1.064$ μm. These values are obtained by rescaling the original values by Singh *et al.*,[19] which were relative to quartz, using a more recently obtained absolute value of quartz recommended by Roberts.[37] For the 311 component, the average was taken of the experimentally slightly different 311 and 113 components. As in the original measurement, we leave the absolute sign undetermined, although the relative sign of the two components was clearly established. By applying Miller's rule[38] that $\chi^{(2)}_{ijk}(-2\omega,\omega,\omega)/\chi^{(1)}_{ii}(2\omega)\chi^{(1)}_{jj}(\omega)\chi^{(1)}_{kk}(\omega)$ is independent of frequency in the low-frequency regime, Chen *et al.*[5] converted these values to $\chi_{333}=\pm 23\pm 3$ and $\chi_{311}=\mp 14\pm 2$ pm/V in the zero-frequency limit. Our LDA values are apparently closer to these values than the scissor corrected values. As noted earlier, we expect our scissor values to be overcorrected because of both the intrinsic problem of the scissor's approach and our use of the actual gap correction rather than a scaled down value that would reproduce the magnitude of $\varepsilon_1(0)$.

Somewhat different experimental values were determined by Lundquist *et al.*[22,23] for $6H$ bulk samples and $6H$ thin films, respectively. Their second set of values is reasonably close to ours in magnitude but shows a ratio of χ_{333}/χ_{311} of -3.[23] The older data[22] are about a factor 2.5 larger for the 333 component and the above ratio was -10. We do not think that crystalline quality alone can explain such large variations. We note that a somewhat indirect fitting procedure was used in these papers in order to determine the ratio of the two components. In an even earlier paper by Harris *et al.*[21] a value smaller by an order of magnitude was obtained for $3C$ SiC films. Because light scattering was a considerable problem in those measurements as the authors state themselves, we can only consider their results as providing a lower limit for the SHG coefficient. Therefore, we chose to compare our calculations only to the older data by Singh *et al.*,[19] in spite of the fact that the polytype was not completely determined in that paper.

We note that the signs of all the components in Table I are opposite to those reported in Ref. 5. The reason for this reversal in the sign of the $\chi^{(2)}$ is simply that opposite coordination of the atomic positions was employed in the two sets of calculations: In $3C$, for example, we placed the Si atom at the (0, 0, 0) and the C atom at the (1/4, 1/4, 1/4) positions in the unit cell, while in Ref. 5 the positions of the Si and the C atoms were interchanged.[39] There were corresponding reversals for the hexagonal polytypes. The agreement in the absolute signs of the $\chi^{(2)}$ components in the two sets of SiC calculations noted above, along with a corresponding agreements for several other semiconductors discussed in our other paper,[1] gives us strong confidence in that regard. However, it appears that the experimental data are still unclear about the sign despite an early effort to determine the absolute sign of the SHG.[20] In that paper a negative sign is proposed for χ_{333} based on a surface etching method for the determination of the crystal orientation. This also coincides with the reported sign of the bond-orbital methods, which, however, could easily give either sign, depending on the details of the model, and is in disagreement with our sign. An unambiguous measurement of the signs, as well as the magnitudes, clearly would be useful.

B. Frequency-dependent results

Figure 2 shows the 333, 311, and 113 components of the $\chi^{(2)}(-2\omega,\omega,\omega)$ for the complete set of SiC polytypes considered here over the energy range 0–8 eV. We note that the hexagonality parameter H decreases monotonically from $2H$ ($H=1$), shown at the top of the figure, to the $3C$ (∞H) polytype ($H=0$) at the bottom. As mentioned above, the ratio of the 333 to the 311 component for $3C$ is the fixed

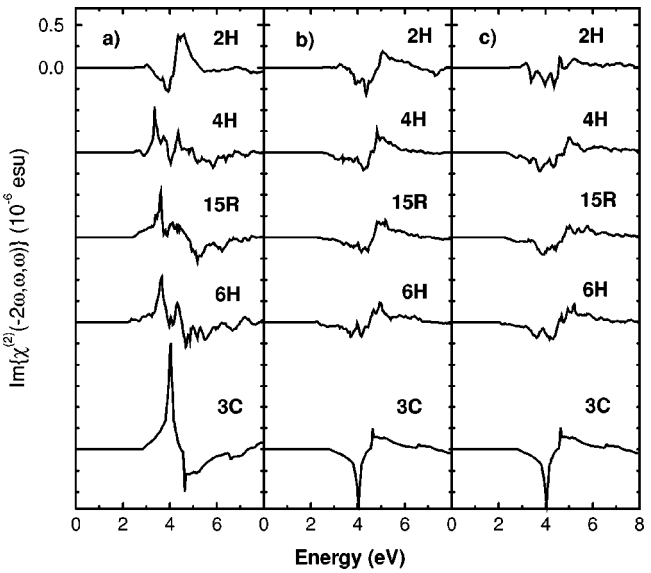

FIG. 2. Calculated values of the imaginary part of $\chi^{(2)}(-2\omega,\omega,\omega)$ for the SiC polytypes considered: (a) 333 component, (b) 311 component, and (c) 113 component.

geometric value of -2. For all other polytypes the ratio is highly frequency dependent in the absorbing frequency regime, i.e., for $\hbar\omega > E_g^d/2$, with E_g^d the smallest direct gap. Below this frequency, the ratio is remarkably constant, as can be seen in Fig. 3. Even in the absorbing frequency range, the ratio of the coefficients averaged over a modest energy of, say, 0.5–1 eV are roughly in the -1 to -2 range with the deviation largest for the largest H, that is, for the wurtzite structure.

It is striking that the 333 component of the wurtzite ($2H$) structure is very different from all other polytypes in that the first peak (at about 4 eV) is negative and the second one positive. In all other polytypes, the first peak is positive and the second negative, with the location of the first peak gradually shifting towards the position of $3C$. In fact, one can see

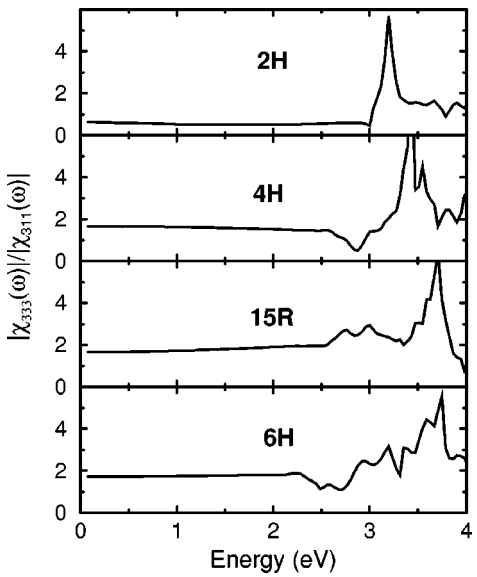

FIG. 3. Ratio $|\chi^{(2)}_{333}(-2\omega,\omega,\omega)|/|\chi^{(2)}_{311}(-2\omega,\omega,\omega)|$ for the noncubic SiC polytypes considered.

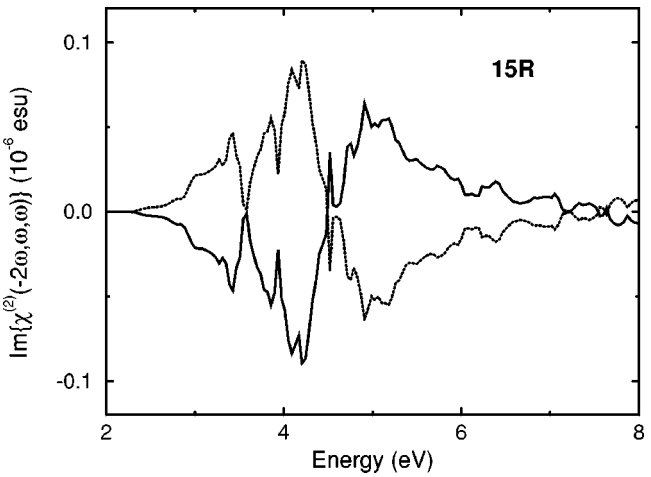

FIG. 4. Calculated 222 (solid line) and 211 (dotted line) components of the imaginary part of the SHG for the rhombohedral 15R polytype. The mirror plane is perpendicular to the x axis.

that the spectra for $4H$, $15R$, and $6H$ show roughly a superposition of the $2H$ and $3C$ characteristic shapes, i.e., they have a $+--+-$ sequence of peaks. One may interpret the first positive peak as cubiclike, the next negative and positive peaks as hexagonal-like, and finally the negative tail appoaching zero as cubiclike. This is not unexpected because the polytypes can be viewed as mixtures of locally cubic and hexagonal stackings. Of course, one cannot push this model too far because the band structures from which the spectra are derived are not simply a superposition of local contributions but contain interference effects of the electron waves. Thus the spectra are not simply a linear superposition in the appropriate ratios of cubic and hexagonal components indicated by the hexagonality.

In the 311 and 113 components, $2H$ appears to be more similar to the other polytypes. Considering the tensorial aspects, one may note the close similarity in spectral features between the 311 and 131 components, which are exactly equal in the static limit.

Also evident in the figures is the general increase in the complexity of the spectral fine structure with decreasing H (or increasing n in the hexagonal nH polytypes) until the cubic structure is reached. This is most clear for the 333 component. This fact clearly reflects the increasing folding of the bands with n or more generally with the size of the basic repeat unit in the stacking sequence. The latter is 2 in $4H$ and 3 in $6H$ because they correspond to bands of two and three consecutive cubically stacked layers alternated with a twin boundary (or hexagonal stacking). In 15R the repeat unit in this sense is $\langle 23\rangle$, although the periodic repeat unit along the c direction is 15 layers. This notation scheme based on the width of the cubically stacked bands is known as the Zhdanov notation.[40] Of course, some of the fine structures exhibited in curves is expected to be averaged out in the observed spectra as a result of broadening effects.

Finally, we consider the additional independent component for the rhombohedral structure. The 222 and 211 components for the 15R polytype are displayed over the range of 2–8 eV in Fig. 4. It is evident that these accurately satisfy the symmetry requirement of having opposite signs. This represents just one more test of the correctness of the code.

The 112 and 121 components were also calculated and, as required, are found to be virtually identical to the 211 component. Finally, we note that the magnitude of these components tends to be smaller than those for the 333 and 311 components by a factor of about 6. These small magnitudes reflect the similarity in the symmetry of the rhombohedral and hexagonal structures.

C. Analysis of SHG spectra

As we noted in another paper,[1] it is convenient to analyze the 2ω- and ω-resonant contributions in the SHG separately as the two parts have features at different energies. A comparison was made there between those two parts and $\varepsilon_2(2\omega)$ and $\varepsilon_2(\omega)$, respectively, for $3C$ SiC (see Fig. 8 of Ref. 1). As might be expected, the location of structures in both parts of $\chi^{(2)}$ coincided with those in the dielectric function. It should be noted that the threshold for the 2ω part occurs at an energy that is half of that for the ω part, E_g^d, which is the direct transition threshold for $\varepsilon_2(\omega)$. As a result, only the 2ω part contributes to $\chi^{(2)}$ in the important energy range $E_g^d/2 < \hbar\omega < E_g^d$. Since $E_g^d \geqslant 6$ eV for the SiC polytypes, unless one is concerned with fairly high energies (well into the UV), the 2ω part is the one of primary interest.

As in $\varepsilon_2(\omega)$, the origin of structure in $\chi^{(2)}$ can be analyzed by a decomposition into separate band-to-band contributions (see, e.g., Ref. 17 for details). The main two peaks in the $\varepsilon_2(\omega)$ curve for $3C$ SiC, for example, result from transitions between the upper valence band to the first and second conduction bands, respectively. Previous analysis shows that the peak with lower energy comes from extended regions of **k** space near the cubic Γ-K-L plane and close to the Γ-L line. The transitions between the same bands and **k**-space regions provide the contributions in the 2ω and ω terms of the $\chi^{(2)}(-2\omega,\omega,\omega)$. These contributions to the total SHG (mostly to its 2ω part in the energy region considered) from these interband transitions are displayed in the top panel of Fig. 5 by the dotted and dashed curves. A similar analysis can be made for $2H$ and the contributions from the relevant interband transitions are similarly indicated in the lower panel of the figure. The major difference between the dielectric function and $\chi^{(2)}$ could loosely be ascribed to the different matrix element factors involved. In the former, only the absolute square of matrix elements occur, ensuring that $\varepsilon_2(\omega)$ is positive. The situation is more complicated for the SHG. Since a complex product of three generally different matrix elements appears in $\chi^{(2)}$, its real and imaginary parts can assume either sign. This is evident in the results for $3C$ and $2H$ shown in Fig. 5.

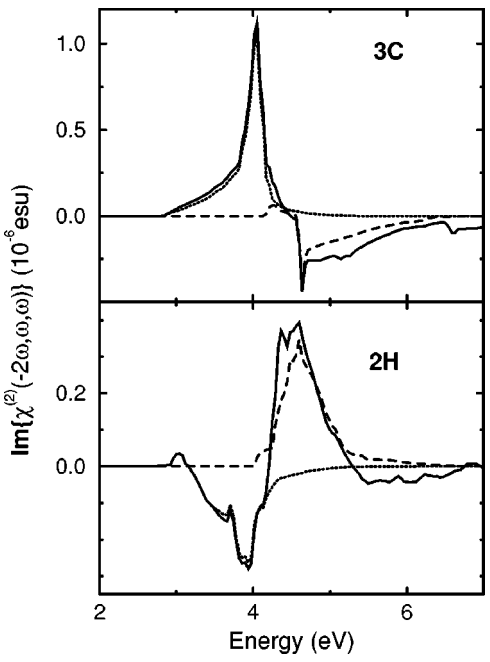

FIG. 5. Top, the analysis of the band-to-band contribution to the 123 component of the SHG for $3C$ SiC: the total SHG (solid line), the upper-valence-band to first-conduction-band contribution (dotted line), and the upper-valence-band to second-conduction-band contribution (dashed line). Bottom, the same for the $2H$ polytype (333 component): total SHG (solid line), the two-upper-valence-band to first- and second-conduction-band contribution (dotted line), and the two-upper-valence-band to third- and fourth-conduction-band contribution (dashed line).

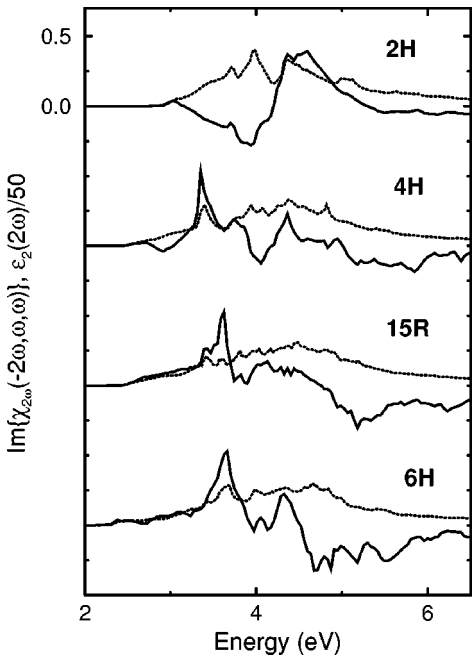

FIG. 6. Values of the 2ω-resonant contributions in the 333 component of the SHG for the noncubic SiC polytypes considered (solid lines), in units 10^{-6} esu, compared with the corresponding $\varepsilon_2^{zz}(2\omega)/50$ (dotted lines).

Similar analyses of the 2ω- and ω-resonant contributions in the SHG have been also performed for the other SiC polytypes. Comparisons between the z-polarized component of the dielectric functions (DF's) and the 333 components of the SHG for the $2H$, $4H$, $15R$, and $6H$ polytypes are shown in Figs. 6 and 7. These components involve the same (z-polarized) momentum matrix element. This guarantees that the selection rules for a given electronic transition will be the same for both curves. Again, all the transitions (including those with rather small oscillator strength) are seen in both the DF and SHG curves and the 2ω part of the SHG dominates in the whole frequency range considered in Fig. 6. The imaginary parts of the DF's look rather similar for all the polytypes and differ from each other only in some fine

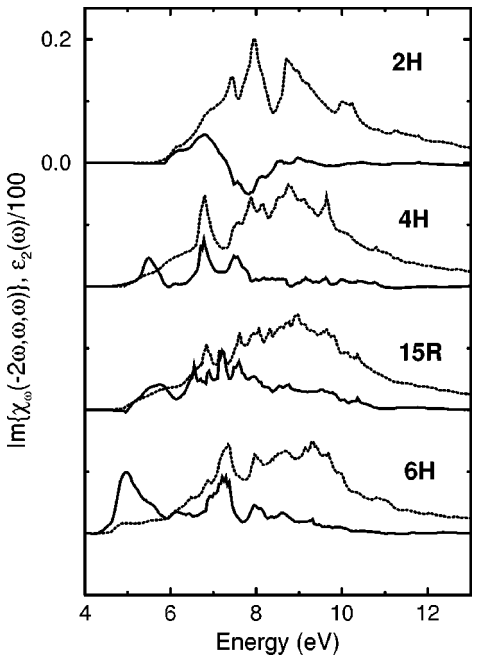

FIG. 7. Values of the ω-resonant contributions in the 333 component of the SHG for the noncubic SiC polytypes considered (solid lines), in units 10^{-6} esu, compared with the corresponding $\varepsilon_2^{zz}(\omega)/100$ (dotted lines).

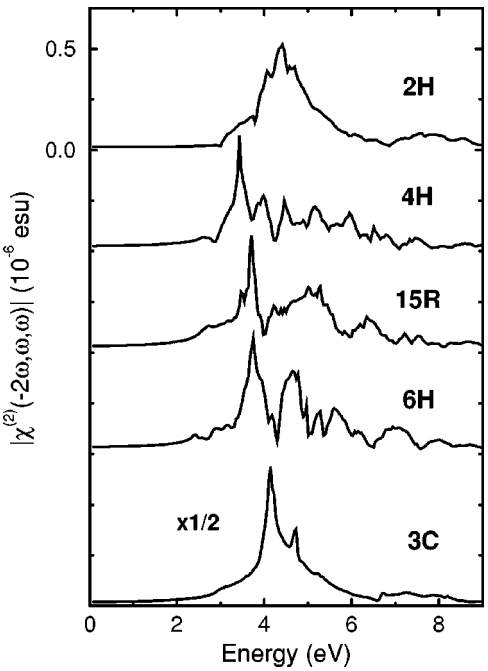

FIG. 8. Absolute values of the frequency-dependent 333 component of the SHG for the SiC polytypes considered.

details, except for the pure hexagonal polytype $2H$. However, the SHG's contain many more features and their changes from polytype to polytype are much more dramatic. This reflects the fact that the electronic structure for the higher polytypes becomes more and more complicated with increasing n. This results in part from the above-mentioned fact that the number of bands increases because of the effects of the band foldings (for layers with cubic stackings) and also from the appearance of the new local symmetries (for hexagonal stackings). Concomitantly, the analysis of the band-to-band contributions becomes increasingly complicated. For the pure hexagonal polytype $2H$, however, we see that the 333 component consists of two wide strips, one between 3 eV and 4.3 eV and the other between 4.3 eV and 5.2 eV. The former results from transitions from the two upper valence bands to the first and second conduction bands and the latter from transitions to the third and fourth conduction bands (see Fig. 5). The matrix element factor for the first strip is negative, while that for the second one is positive. This is opposite to the case of $3C$ SiC, where the lower-energy peak is positive. This large negative feature of the 333 component near the threshold $E_g^d/2$ is unique to the $2H$ polytype, as was mentioned before.

Figure 8 shows the absolute value of the frequency-dependent 333 component of $\chi^{(2)}$ for the four noncubic polytypes. The reported measurements of frequency-dependent results for other materials have generally been only for the absolute values of the SHG rather than the real or imaginary parts. Consequently, the numerical calculations of this function are of interest for future comparisons to experimental data. It can be seen that the line shape of the $|\chi^{(2)}(-2\omega,\omega,\omega)|$ for the pure hexagonal $2H$ material again exhibits the greatest differences from those of the other polytypes. Another interesing feature of $|\chi^{(2)}(-2\omega,\omega,\omega)|$ for $2H$ is its very weak dispersion in the energy interval between zero and $E_g^d/2$; that is, its coefficient of the ω^2 term, which describes the behavior in this region, is much smaller than for the other polytypes. For $4H$, $15R$, and $6H$, the peak between 3 and 4 eV dominates. Its position gradually increases from 3.4 eV for $4H$ to 3.7 eV for $6H$ and to 4.1 eV for $3C$. This structure arises from the 2ω-resonant transitions (see also Fig. 6) and is common for all the polytypes except $2H$.

D. Near-band-edge fine structure

An interesting feature of the various SHG spectra displayed in the previous sections is the appearance of considerable fine structure in the energy region between the threshold for the direct interband transitions and the dominant peak around 3.5 eV. These structures, if detectable, could provide important information about the conduction- and valence-band edges. Neither the presently available reflectivity spectra[17] nor the measurements of the dielectric function by spectroscopic ellipsometry[41] had the required resolution to provide such detailed information about this region of the spectra.

However, that information could be quite useful for determining the nature of the band edges and hence for an understanding of the conduction properties in doped SiC polytypes. Information about the band edges has previously been obtained by different methods. These include analyses of the optically detected cyclotron resonances[42] and of the phonon replica spectra associated with donor-bound excitons. The latter are due to the phonons, which have a wave vector equal to the **k**-point location of the conduction-band minimum.[43,44] These analyses led to the conclusion that the minimum of the conduction band in $4H$ is at the M point of the BZ, in agreement with the predictions of the band calculations. For $6H$ the situation is more complicated because not all of the multitude of phonon lines have as yet been

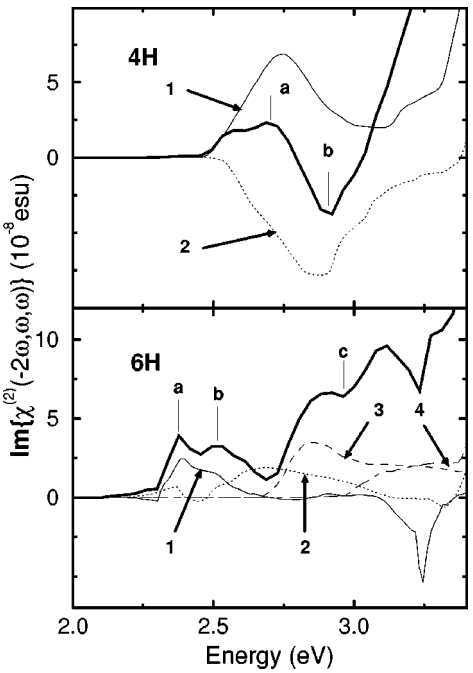

FIG. 9. Analysis of the band-to-band contributions to $\mathrm{Im}\{\chi^{(2)}_{333}(-2\omega,\omega,\omega)\}$ in the energy region associated with the direct transitions between the near ''band edges'' for the $4H$ and $6H$ polytypes. The totals are given by the thick solid lines and the numbers labeling the curves for the partial band-to-band contribution correspond to the interband transitions indicated in Fig. 10.

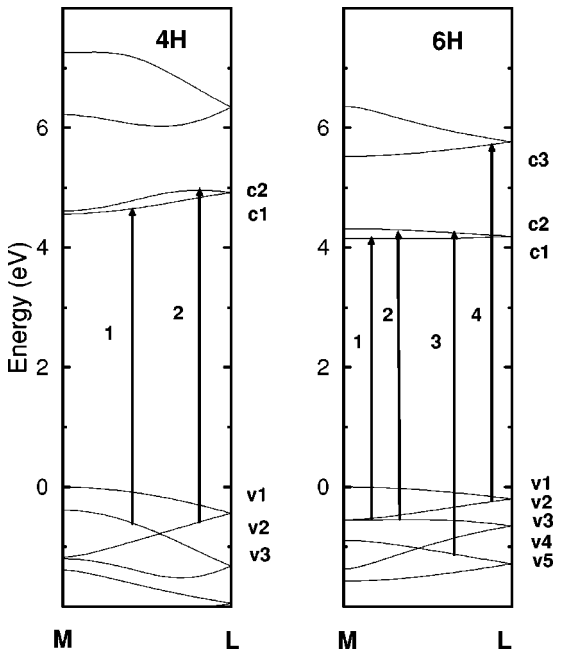

FIG. 10. Electronic band structures for the $4H$ and $6H$ polytypes along the M-L line of the BZ. The LDA conduction bands are shifted up by a 1-eV ''correction.'' The transitions associated with the important contributions to the SHG (and displayed in Fig. 9) are indicated by arrows.

resolved and also because of the believed shallow nature of the minimum itself. In another experiment, the optical transitions from the lowest conduction band to the higher bands were observed in fairly heavily n-type doped samples.[45] These spectra were recently analyzed by Lambrecht *et al.*[46]

The direct measurements of the SHG in this energy region could provide additional information about the bands in the first few eV from the band edges. Figure 9 shows the analysis of the band-to-band contribution to the 2ω term in the imaginary part of the SHG (333 component) for $4H$ and $6H$ polytypes. We analyze $\mathrm{Im}\{\chi^{(2)}(-2\omega,\omega,\omega)\}$, but, of course, the same features would appear in $|\chi^{(2)}(-2\omega,\omega,\omega)|$. For both polytypes the behavior of the SHG in this region is determined by the transitions near the M point (see Fig. 10). For $4H$, the structure of $\mathrm{Im}\{\chi^{(2)}(-2\omega,\omega,\omega)\}$ between 2.5 and 3 eV results from transitions between the valence band $v2$ and the two lowest conduction bands ($c1$ and $c2$). The transitions to the first conduction band produce a positive contribution to the SHG, while those to the second band are negative. The separation between the broad maximum of SHG around 2.7 eV (the **a** feature) and the minimum at 2.9 eV (the **b** feature) is thus closely related to the energy difference between the two lowest conduction bands and the dispersion of the second highest valence band along the M-L line (Fig. 10). Although the relation is not simple, it illustrates that we can relate the features of the SHG curve to specific band-to-band contributions.

The situation in $6H$ is more complicated. The total SHG curve in this region exhibits more structure than for $4H$. The lower peak at 2.38 eV (the **a** feature) results mainly from transitions between the two valence bands $v2$ and $v3$ and the lowest conduction band $c1$ (arrow 1 in the right-hand panel of Fig. 10). The partial contribution from these transitions decreases and changes sign at higher energy and ultimately produces a sharp minimum at 3.25 eV. This behavior is also reflected in the total curve. The second (**b**) structure at 2.51 eV results from the superposition of the first curve and the contribution from transitions from the same valence bands ($v2$ and $v3$) to the second conduction band $c2$ (arrow 2). The broad hump that starts at 2.75 eV originates from transitions between the rather low-lying valence band $v5$ and the second conduction band $c2$ (arrow 3). The last interesting feature to be discussed is the hump starting at 2.95 eV (the **c** feature). This structure is associated with transitions between the two upper valence bands ($v1$ and $v2$) and the third conduction band $c3$ (arrow 4). While the total curve is fairly complicated, we see that energy differences in its features can be approximately related to half the differences between the interband transition energies (Fig. 10).

IV. CONCLUSIONS

The second-harmonic generation coefficients for five important SiC polytypes $3C$, $6H$, $15R$, $4H$, and $2H$ have been calculated over the energy range from 0 to 13 eV. The results for the zero-frequency limit of the ratios of the 333 and 311 components are in good agreement with those obtained in pseudopotential calculations,[5] while the magnitudes of the individual components are found to be smaller than those reported earlier. The polytypes studied span the full range of hexagonality from zero for $3C$ to unity (complete hexagonality) for $2H$ SiC. This allowed for a study of the trends in the SHG with this quantity, which characterizes the polytypes. It is found that with the exception of the 333 component of $2H$ SiC, the frequency-dependent SHG coefficients

in the different polytypes look rather similar over a broad frequency range. The spectra gradually approach those for the zinc-blende $3C$ polytype but exhibit increasing complexity with increasing length of the basic repeat unit of the layer stackings. All independent tensor components were obtained (and their symmetry relations verified), including the small ones that are are only nonvanishing in the rhombohedral case. We also find that the components that are strictly equal in the static limit by the Kleinman symmetry still show great similarity over the full frequency range. The spectral features in the 333 component were further analyzed by examining separately the ω and 2ω resonances, the absolute values, and their correspondence to features in the 33 component of the imaginary part of the dielectric function. These one-to-one correspondences and further explicit decompositions allowed us to assign the spectral features to specific band-to-band contributions. We carried this out in considerable detail for the transitions in $4H$ and $6H$ in the low-energy region, which is the most accessible region experimentally.

An important general conclusion of this last aspect of our work is that the frequency-dependent $\chi^{(2)}$ may provide a useful tool for studying the electronic structure especially for the wide-band-gap semiconductors. This is particularly important for studying the bands in the vicinity of the band edges. To our knowledge this has not been done before. The observation of structure in the linear-response functions arising from direct transitions involving these band edges is hindered by the weakness of those features. They probably can be seen in derivative spectra of the DF, i.e., by modulation spectroscopy. In some sense, SHG provides information similar to that obtained from the modulation spectroscopies. For the SiC polytypes (and other wide-band-gap semiconductors as well) the measurements of the 2ω part of the SHG involving the near band edges lie in the visible light region where available lasers can be employed. In spite of the fact that the amplitudes of the features to be detected are rather small, they are comparable to the zero-frequency limits of the SHG that have been measured. This implies that they can be experimentally detected.

ACKNOWLEDGMENTS

Part of the computations were performed at the Ohio Supercomputer Center. This work was supported by NSF Grant No. DMR95-29376.

*Permanent address: P. N. Lebedev Physical Institute, Russian Academy of Sciences, 117924 Moscow, Russian Federation.

[1] S. N. Rashkeev, W. R. L. Lambrecht, and B. Segall, Phys. Rev. B **57**, 3905 (1998).

[2] J. L. P. Hughes and J. E. Sipe, Phys. Rev. B **53**, 10 751 (1996).

[3] J. L. P. Hughes, Y. Wang, and J. E. Sipe, Phys. Rev. B **55**, 13 630 (1997).

[4] Z. H. Levine and D. C. Allan, Phys. Rev. B **43**, 4187 (1991); **44**, 12 781 (1991); Z. H. Levine, Int. J. Quantum Chem. **S28**, 411 (1991).

[5] J. Chen, Z. H. Levine, and J. W. Wilkins, Phys. Rev. B **50**, 11 514 (1994).

[6] J. Chen, Z. H. Levine, and J. W. Wilkins, Appl. Phys. Lett. **66**, 1129 (1995).

[7] J. E. Sipe and E. Ghahramani, Phys. Rev. B **48**, 11 705 (1993).

[8] C. Aversa and J. E. Sipe, Phys. Rev. B **52**, 14 636 (1995).

[9] R. M. Martin, Phys. Rev. B **6**, 4546 (1972).

[10] K. Kim, W. R. L. Lambrecht, and B. Segall, Phys. Rev. B **53**, 16 310 (1996); **56**, 7018 (1997).

[11] B. F. Levine, Phys. Rev. Lett. **25**, 440 (1970).

[12] A. P. Verma and P. Krishna, *Polymorphism and Polytypism in Crystals* (Wiley, New York, 1966).

[13] W. R. L. Lambrecht, S. Limpijumnong, S. N. Rashkeev, and B. Segall, Phys. Status Solidi B **202**, 5 (1997).

[14] D. A. Kleinman, Phys. Rev. **126**, 1977 (1962).

[15] Z. Ikonić, G. P. Srivastava, and J. C. Inkson, Phys. Rev. B **48**, 17 181 (1993).

[16] W. H. Backes, P. A. Bobbert, and W. van Haeringen, Phys. Rev. B **49**, 7564 (1994); W. van Haeringen, P. A. Bobbert, and W. H. Backes, Phys. Status Solidi B **202**, 63 (1997).

[17] W. R. L. Lambrecht, B. Segall, M. Yoganathan, W. Suttrop, R. P. Devaty, W. J. Choyke, J. A. Edmond, J. A. Powell, and M. Alouani, Appl. Phys. Lett. **63**, 2747 (1993); Phys. Rev. B **50**, 10 722 (1994).

[18] M. Cardona, *Modulation Spectroscopy* (Academic, New York, 1969).

[19] S. Singh, J. R. Potopowicz, L. G. Van Uitert, and S. H. Wemple, Appl. Phys. Lett. **19**, 53 (1971).

[20] R. C. Miller and W. A. Nordland, Phys. Rev. B **5**, 4931 (1972).

[21] G. L. Harris, E. W. Jones, M. G. Spencer, and K. H. Jackson, Appl. Phys. Lett. **59**, 1817 (1991).

[22] P. M. Lundquist, W. P. Lin, G. K. Wong, M. Razeghi, and J.B. Ketterson, Appl. Phys. Lett. **66**, 1883 (1995); **67**, 2887 (1995).

[23] P. M. Lundquist, H. C. Ong, W. P. Lin, R. P. H. Chang, J.B. Ketterson, and G. K. Wong, Appl. Phys. Lett. **67**, 2919 (1995).

[24] S. Niedermeier, H. Schillinger, S. Karmann, L. Dressler, K. Goetz, W. Richter, and R. Sauerbrey (unpublished).

[25] O. K. Andersen, Phys. Rev. B **12**, 3060 (1975).

[26] O. K. Andersen, O. Jepsen, and M Šob, in *Electronic Band Structure and Its Applications*, edited by M. Yussouf (Springer, Heidelberg, 1987), p. 1.

[27] W. Kohn and L. J. Sham, Phys. Rev. **140**, A1133 (1965).

[28] L. Hedin and B. I. Lundqvist, J. Phys. C **4**, 2064 (1971).

[29] W. G. Aulbur, L. Jönsson, and J. W. Wilkins, Phys. Rev. B **54**, 8540 (1996).

[30] L. Hedin and S. Lundqvist, in *Solid State Physics, Advances in Research and Applications*, edited by F. Seitz, D. Turnbull, and H. Ehrenreich (Academic, New York, 1969), Vol. 23, p. 1.

[31] V. I. Gavrilenko and F. Bechstedt, Phys. Rev. B **54**, 13 416 (1996).

[32] M. Rohlfing, P. Krüger, and J. Pollmann, Phys. Rev. B **48**, 17 791 (1993).

[33] W. H. Backes, P. A. Bobbert, and W. van Haeringen, Phys. Rev. B **51**, 4950 (1994).

[34] B. Wenzien, P. Käckell, F. Bechstedt, and G. Cappellini, Phys. Rev. B **52**, 10 897 (1995).

[35] D. A. Kleinman, Phys. Rev. B **2**, 3139 (1970).

[36] It was clearly an α-form of SiC, i.e., not cubic. According to Singh *et al.* (Ref. 19), it was hexagonal and not rhombohedral because of the absence of the χ_{222} component. Our present calculations, however, indicate that χ_{222} is quite small and hence might have been missed. According to Miller and Nordland

(Ref. 20), it was probably 15*R* based on the birefringence data.
[37] D. A. Roberts, IEEE J. Quantum Electron. **28**, 2057 (1992).
[38] R. C. Miller, Appl. Phys. Lett. **5**, 17 (1964).
[39] J. Chen (private communication).
[40] G. S. Zhdanov, C. R. Acad.. Sci. USSR **48**, 43 (1945).
[41] S. Logothetidis, H. M. Polatoglou, J. Petalas, D. Fuchs, and R. L. Johnson, Physica B **185**, 389 (1993).
[42] W. R. L. Lambrecht and B. Segall, Phys. Rev. B **52**, R2249 (1995).
[43] L. Patrick, W. J. Choyke, and D. R. Hamilton, Phys. Rev. **137**, A1515 (1965).
[44] W. J. Choyke, R. P. Devaty, L. L. Clemen, M. F. MacMillan, and Y. Yoganathan, in *Silicon Carbide and Related Materials*, Proceedings of the Sixth International Conference on Silicon Carbide and Related Materials, Kyoto, Japan, 1995, edited by S. Nakashima, H. Matsunami, S. Yoshida, and H. Harima, IOP Conf. Proc. No. 142 (Institute of Physics and Physical Society, Bristol, 1996), p. 257.
[45] E. Biedermann, Solid State Commun. **3**, 343 (1965).
[46] W. R. L. Lambrecht, S. Limpijumnong, S. N. Rashkeev, and B. Segall, in Proceedings of the International Conference on Silicon Carbide, III-Nitrides and Related Materials, Stockholm, 1997, edited by G. Pensl, H. Morkoc, B. Monemar, and E. Janzon (Trans Tech, Aedermannsdorf, in press).